ViTGAN: Training GANs with Vision Transformers

Kwonjoon Lee[1]   Huiwen Chang[2]   Lu Jiang[2]   Han Zhang[2]
Zhuowen Tu[1]   Ce Liu[2]

[1]UC San Diego   [2]Google Research

{kwl042,ztu}@ucsd.edu   {huiwenchang,lujiang,zhanghan,celiu}@google.com

Abstract

Recently, Vision Transformers (ViTs) have shown competitive performance on image recognition while requiring less vision-specific inductive biases. In this paper, we investigate if such observation can be extended to image generation. To this end, we integrate the ViT architecture into generative adversarial networks (GANs). We observe that existing regularization methods for GANs interact poorly with self-attention, causing serious instability during training. To resolve this issue, we introduce novel regularization techniques for training GANs with ViTs. Empirically, our approach, named *ViTGAN*, achieves comparable performance to state-of-the-art CNN-based StyleGAN2 on CIFAR-10, CelebA, and LSUN bedroom datasets.

1   Introduction

Convolutional neural networks (CNNs) [31] are dominating computer vision today, thanks to their powerful capability of convolution (weight-sharing and local-connectivity) and pooling (translation equivariance). Recently, however, Transformer architectures [55] have started to rival CNNs in image [9, 15, 51] and video [5, 3] recognition tasks. In particular, Vision Transformers (ViTs) [15], which interprets an image as a sequence of *tokens* (analogous to *words* in natural language), has been shown by Dosovitskiy *et al*. to achieve comparable classification accuracy with smaller computational budgets (*i.e*., fewer FLOPs) on the ImageNet benchmark. Different from local-connectivity in CNNs, ViTs rely on globally-contextualized representation where each patch is attended to *all* patches of the same image. ViTs, along with their variants [51, 50], though still in their infancy, have demonstrated promising advantages in modeling non-local contextual dependencies [42, 48] as well as excellent efficiency and scalability. Since its recent inception, ViTs have been used in various other tasks such as object detection [4], video recognition [5, 3], multitask pretraining [8], *etc*.

In this paper, we are interested in examining whether the task of image generation can be achieved by Vision Transformers *without using convolution or pooling*, and more specifically, whether ViTs can be used to train generative adversarial networks (GANs) with competitive quality to well-studied CNN-based GANs. To this end, we train GANs with Vanilla-ViT (as in Fig. 2 (A)) following the design of the original ViT [15]. The challenge is that GAN training becomes highly unstable when coupled with ViTs, and that adversarial training is frequently hindered by high-variance gradients (or spiking gradients) in the later stage of discriminator training. Furthermore, conventional regularization methods such as gradient penalty [19, 33], spectral normalization [35] cannot resolve the instability issue even though they are proved to be effective for CNN-based GAN models (shown in Fig. 4). As unstable training is uncommon in the CNN-based GANs training with appropriate regularization, this presents a unique challenge to the design of ViT-based GANs.

Hence, in this paper, we propose several necessary modifications to stabilize the training dynamics and facilitate convergence of ViT-based GANs. In the *discriminator*, we revisit the Lipschitz property of self-attention [28], and further design an improved spectral normalization that enforces
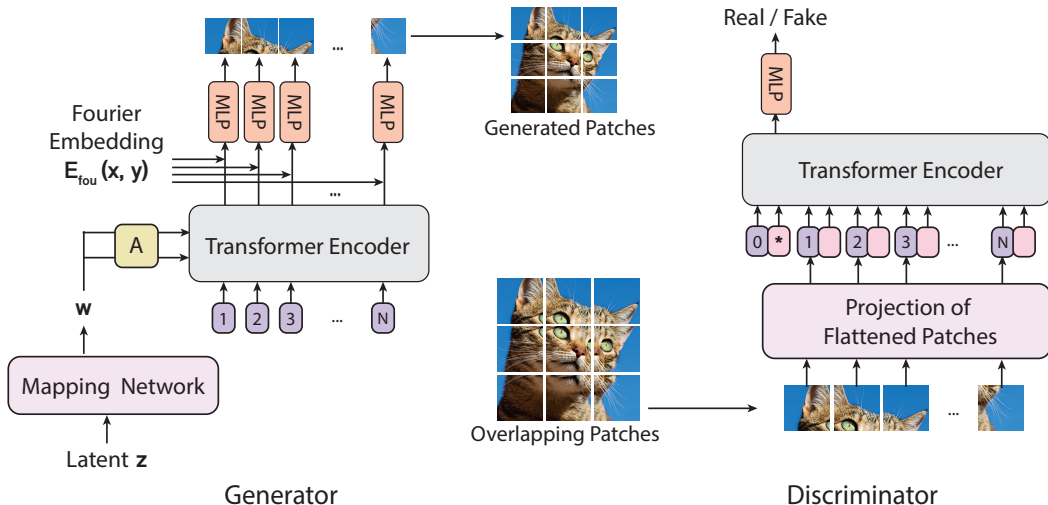
Figure 1: **Overview of the proposed ViTGAN framework.** Both the generator and the discriminator are designed based on the Vision Transformer (ViT). Discriminator score is derived from the classification embedding (denoted as [*] in the Figure). The generator generates pixels patch-by-patch based on patch embeddings.

Lipschitz continuity. Different from the conventional spectral normalization, which fails to resolve the instability issue, these techniques exhibit high efficacy in stabilizing the training dynamics of the ViT-based discriminators. We conduct ablation studies (Fig. 4 and Table 3b) to validate the necessity of the proposed techniques and their central role in achieving stable and superior image generation performance. For the ViT-based *generator*, we study a variety of architecture designs and discover two key modifications to the layer normalization and output mapping layers. Experiments show that the modified ViT-based generator can better facilitate the adversarial training with both ViT-based and CNN-based discriminators.

We perform experiments on three standard image synthesis benchmarks. The results show that our model, named *ViTGAN*, outperforms the previous Transformer-based GAN model [23] by a large margin, and achieves comparable performance to leading CNN-based GANs such as Style-GAN2 [27], even *without using convolution or pooling*. To the best of our knowledge, the proposed ViTGAN model is among the first approaches that leverage Vision Transformers in GANs, and more importantly, the first to demonstrate such Transformer's comparable performance over the state-of-the-art convolutional architecture [27, 6] on standard image generation benchmarks including CIFAR, CelebA, and LSUN bedroom datasets.

2   Related Work

Generative Adversarial Networks   Generative adversarial networks (GANs) [18] model the target distribution using adversarial learning. It is typically formulated as a min-max optimization problem minimizing some distance between the real and generated data distributions, *e.g.*, through various f-divergences [38] or integral probability metrics (IPMs) [37, 47] such as the Wasserstein distance [2].

The GAN models are notorious for unstable training dynamics. As a result, numerous efforts have been proposed aiming at stabilizing training, thereby ensuring convergence. Common approaches include spectral normalization [35], gradient penalty [19, 33, 29], consistency regularization [58, 60], and data augmentation [59, 25, 61, 52]. These techniques are all designed inside convolutional neural networks (CNN) and have been only verified in the convolutional GAN models. However, we find that these methods are insufficient for stabilizing the training of Transformer-based GANs. A similar finding was reported in [11] on a different task of pretraining. This may stem from ViTs' exceeding capability [15] and capturing of a different type of inductive bias than CNN via self-

attention [28, 14, 12]. This paper introduces novel techniques to overcome the unstable adversarial training of Vision Transformers.

Vision Transformers Vision Transformer (ViT) [15] is a convolution-free Transformer that performs image classification over a sequence of image patches. ViT demonstrates the superiority of the Transformer architecture over the classical CNNs by taking advantage of pretraining on large-scale datasets. Afterward, DeiT [51] improves ViTs' sample efficiency by knowledge distillation as well as regularization tricks. MLP-Mixer [50] further drops self-attention and replaces it by an MLP to mix the per-location feature. In parallel, ViT has been extended to various computer vision tasks such as object detection [4], action recognition in video [5, 3], multitask pretraining [8]. Our work is among the first to exploit Vision Transformers in the GAN model for image generation.

Generative Transformer in Vision Motivated by the success of GPT-3 [7], a few pilot works study image generation using Transformer by autoregressive learning [9, 16] or cross-modal learning between image and text [41]. These methods are different from ours as they model image generation as a autoregressive sequence learning problem. On the contrary, our work trains Vision Transformers in the generative adversarial training paradigm. The closest work to ours is TransGAN [23], presenting a pure transformer based GAN model. While proposing multi-task co-training and localized initialization for better training, TransGAN neglects key techniques for training stability and underperforms the leading convolutional GAN models by a considerable margin. By virtue of our design, this paper is the first to demonstrate Transformer-based GANs are able to achieve competitive performance compared to state-of-the-art CNN-based GAN models.

3   Preliminaries: Vision Transformers (ViTs)

Vision Transformer [15] is a pure transformer architecture for image classification that operates upon a sequence of image patches. The 2D image $\mathbf{x} \in \mathbb{R}^{H \times W \times C}$ is flattened into a sequence of image patches, following the raster scan, denoted by $\mathbf{x}_p \in \mathbb{R}^{L \times (P^2 \cdot C)}$, where $L = \frac{H \times W}{P^2}$ is the effective sequence length and $P \times P \times C$ is the dimension of each image patch.

Following BERT [13], a learnable classification embedding $\mathbf{x}_{\text{class}}$ is prepended to the image sequence along with the added 1D positional embeddings $\mathbf{E}_{pos}$ to formulate the patch embedding $\mathbf{h}_0$. The architecture of ViT closely follows the Transformer architecture [55].

$$\mathbf{h}_0 = [\mathbf{x}_{\text{class}}; \mathbf{x}_p^1 \mathbf{E}; \mathbf{x}_p^2 \mathbf{E}; \cdots ; \mathbf{x}_p^L \mathbf{E}] + \mathbf{E}_{pos}, \qquad \mathbf{E} \in \mathbb{R}^{(P^2 \cdot C) \times D}, \mathbf{E}_{pos} \in \mathbb{R}^{(L+1) \times D} \quad (1)$$

$$\mathbf{h}'_\ell = \text{MSA}(\text{LN}(\mathbf{h}_{\ell-1})) + \mathbf{h}_{\ell-1}, \qquad\qquad \ell = 1, \ldots, L \quad\quad (2)$$

$$\mathbf{h}_\ell = \text{MLP}(\text{LN}(\mathbf{h}'_\ell)) + \mathbf{h}'_\ell, \qquad\qquad\qquad \ell = 1, \ldots, L \quad\quad (3)$$

$$\mathbf{y} = \text{LN}(\mathbf{h}_L^0) \qquad\qquad\qquad\qquad\qquad\qquad\qquad (4)$$

Equation 2 applies multi-headed self-attention (MSA). Given learnable matrices $\mathbf{W}_q, \mathbf{W}_k, \mathbf{W}_v$ corresponding to query, key, and value representations, a single self-attention head (indexed with h) is computed by:

$$\text{Attention}_h(\mathbf{X}) = \text{softmax}\Big(\frac{\mathbf{Q}\mathbf{K}^\top}{\sqrt{d_h}}\Big)\mathbf{V}, \qquad\qquad (5)$$

where $\mathbf{Q} = \mathbf{X}\mathbf{W}_q$, $\mathbf{K} = \mathbf{X}\mathbf{W}_k$, and $\mathbf{V} = \mathbf{X}\mathbf{W}_v$. Multi-headed self-attention aggregates information from H self-attention heads by means of concatenation and linear projection, as follows:

$$\text{MSA}(\mathbf{X}) = \text{concat}_{h=1}^{H}[\text{Attention}_h(\mathbf{X})]\mathbf{W} + \mathbf{b}. \qquad\qquad (6)$$

4   Method

Fig. 1 illustrates the architecture of the proposed ViTGAN with a ViT discriminator and a ViT-based generator. We find that directly using ViT as the discriminator makes the training volatile. We introduce techniques to both generator and discriminator to stabilize the training dynamics and facilitate the convergence: *(1)* regularization on ViT discriminator and *(2)* new architecture for generator.

3

4.1 Regularizing ViT-based discriminator

Enforcing Lipschitzness of Transformer Discriminator Lipschitz continuity plays a critical role in GAN discriminators. It was first brought to attention as a condition to approximate the Wasserstein distance in WGAN [2], and later was confirmed in other GAN settings [17, 35, 57] beyond the Wasserstein loss. In particular, [62] proves that Lipschitz discriminator guarantees the existence of the optimal discriminative function as well as the existence of a unique Nash equilibrium. A very recent work [28], however, shows that Lipschitz constant of standard dot product self-attention (*i.e.*, Equation 5) layer can be unbounded, rendering Lipschitz continuity violated in ViTs. To enforce Lipschitzness of our ViT discriminator, we adopt *L2 attention* proposed in [28]. As shown in Equation 7, we replace the dot product similarity with Euclidean distance and also tie the weights for the projection matrices for query and key in self-attention:

$$\text{Attention}_h(\mathbf{X}) = \text{softmax}\Big(\frac{d(\mathbf{X}\mathbf{W}_q, \mathbf{X}\mathbf{W}_k)}{\sqrt{d_h}}\Big)\mathbf{X}\mathbf{W}_v, \quad \text{where} \quad \mathbf{W}_q = \mathbf{W}_k, \tag{7}$$

$\mathbf{W}_q$, $\mathbf{W}_k$, and $\mathbf{W}_v$ are the projection matrices for query, key, and value, respectively. $d(\cdot, \cdot)$ computes *vectorized L2 distances* between two sets of points. $\sqrt{d_h}$ is the feature dimension for each head. This modification improves the stability of Transformers when used for GAN discriminators.

Improved Spectral Normalization. To further strengthen the Lipschitz continuity, we also apply spectral normalization (SN) [35] in the discriminator training. The standard SN uses power iterations to estimate spectral norm of the projection matrix for each layer in the neural network. Then it divides the weight matrix with the estimated spectral norm, so Lipschitz constant of the resulting projection matrix equals 1. We find Transformer blocks are sensitive to the scale of Lipschitz constant, and the training exhibits very slow progress when the SN is used (*c.f.* Table 3b). Similarly, we find R1 gradient penalty cripples GAN training when ViT-based discriminators are used (*c.f.* Figure 4). [14] suggests that the small Lipschitz constant of MLP block may cause the output of Transformer collapse to a rank-1 matrix. To resolve this, we propose to increase the spectral norm of the projection matrix.

We find that multiplying the normalized weight matrix of each layer with the **spectral norm at initialization** is sufficient to solve this problem. Concretely, we use the following update rule for our spectral normalization, where σ computes the standard spectral norm of weight matrices:

$$\bar{W}_{\text{ISN}}(\mathbf{W}) := \sigma(\mathbf{W}_{init}) \cdot \mathbf{W}/\sigma(\mathbf{W}). \tag{8}$$

Overlapping Image Patches. ViT discriminators are prone to overfitting due to their exceeding learning capacity. Our discriminator and generator use the same image representation that partitions an image as a sequence of non-overlapping patches according to a predefined grid $P \times P$. These arbitrary grid partitions, if not carefully tuned, may encourage the discriminator to memorize local cues and stop providing meaningful loss for the generator. We use a simple trick to mitigate this issue by allowing some overlap between image patches. For each border edge of the patch, we extend it by o pixels, making the effective patch size $(P + 2o) \times (P + 2o)$.

This results in a sequence with the same length but less sensitivity to the predefined grids. It may also give the Transformer a better sense of which ones are neighboring patches to the current patch, hence giving a better sense of locality.

4.2 Generator Design

Designing a generator based on the ViT architecture is a nontrivial task. A challenge is converting ViT from predicting a set of class labels to generating pixels over a spatial region. Before introducing our model, we discuss two plausible baseline models, as shown in Fig. 2 (A) and 2 (B). Both models swap ViT's input and output to generate pixels from embeddings, specifically from the latent vector $\mathbf{w}$ derived from a Gaussian noise vector $\mathbf{z}$ by an MLP, *i.e.*, $\mathbf{w} = \text{MLP}(\mathbf{z})$ (called mapping network [26] in Fig. 2). The two baseline generators differ in their input sequences. Fig. 2 (A) takes as input a sequence of positional embeddings and adds the intermediate latent vector $\mathbf{w}$ to every positional embedding. Alternatively, Fig. 2 (B) prepends the sequence with the latent vector. This design is inspired by inverting ViT where $\mathbf{w}$ is used to replace the classification embedding $\mathbf{h}_L^0$ in Equation 4.
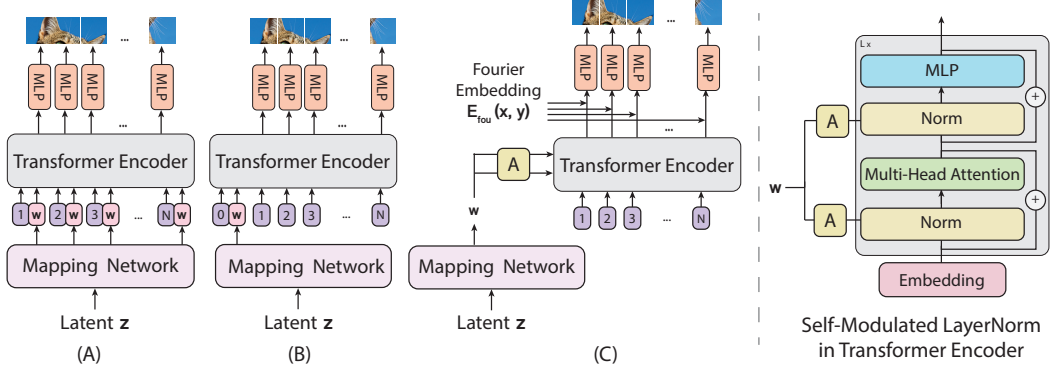
4

Figure 2: **Generator Architectures.** The diagram on the left shows three generator architectures we consider: **(A)** adding intermediate latent embedding **w** to every positional embedding, **(B)** prepending **w** to the sequence, and **(C)** replacing normalization with self-modulated layernorm (SLN) computed by learned affine transform (denoted as **A** in the figure) from **w**. On the right, we show the details of the self-modulation operation applied in the Transformer block.

To generate pixel values, a linear projection $\mathbf{E} \in \mathbb{R}^{D \times (P^2 \cdot C)}$ is learned in both models to map a D-dimensional output embedding to an image patch of shape $P \times P \times C$. The sequence of $L = \frac{H \times W}{P^2}$ image patches $[\mathbf{x}_p^i]_{i=1}^L$ are finally reshaped to form an whole image $\mathbf{x}$.

These baseline transformers perform poorly compared to the CNN-based generator. We propose a novel generator following the design principle of ViT. Our ViTGAN Generator, shown in Fig. 2 (c), consists of two components (1) a transformer block and (2) an output mapping layer.

$$\mathbf{h}_0 = \mathbf{E}_{pos}, \qquad\qquad\qquad \mathbf{E}_{pos} \in \mathbb{R}^{L \times D}, \qquad\qquad (9)$$

$$\mathbf{h'}_\ell = \mathrm{MSA}(\mathrm{SLN}(\mathbf{h}_{\ell-1}, \mathbf{w})) + \mathbf{h}_{\ell-1}, \qquad \ell = 1, \ldots, L, \mathbf{w} \in \mathbb{R}^D \qquad (10)$$

$$\mathbf{h}_\ell = \mathrm{MLP}(\mathrm{SLN}(\mathbf{h'}_\ell, \mathbf{w})) + \mathbf{h'}_\ell, \qquad \ell = 1, \ldots, L \qquad\qquad (11)$$

$$\mathbf{y} = \mathrm{SLN}(\mathbf{h}_L, \mathbf{w}) = [\mathbf{y}^1, \cdots, \mathbf{y}^L] \qquad \mathbf{y}^1, \ldots, \mathbf{y}^L \in \mathbb{R}^D \qquad (12)$$

$$\mathbf{x} = [\mathbf{x}_p^1, \cdots, \mathbf{x}_p^L] = [f_\theta(\mathbf{E}_{fou}, \mathbf{y}^1), \ldots, f_\theta(\mathbf{E}_{fou}, \mathbf{y}^L)] \quad \mathbf{x}_p^i \in \mathbb{R}^{P^2 \times C}, \mathbf{x} \in \mathbb{R}^{H \times W \times C} \quad (13)$$

The proposed generator incorporates two modifications to facilitate the training.

Self-modulated LayerNorm. Instead of sending the noise vector **z** as the input to ViT, we use **z** to modulate the layernorm operation in Equation 10. This is known as self-modulation [10] since the modulation depends on no external information. The self-modulated layernorm (SLN) in Equation 10 is computed by:

$$\mathrm{SLN}(\mathbf{h}_\ell, \mathbf{w}) = \mathrm{SLN}(\mathbf{h}_\ell, \mathrm{MLP}(\mathbf{z})) = \gamma_\ell(\mathbf{w}) \odot \frac{\mathbf{h}_\ell - \boldsymbol{\mu}}{\boldsymbol{\sigma}} + \beta_\ell(\mathbf{w}), \qquad (14)$$

where $\boldsymbol{\mu}$ and $\boldsymbol{\sigma}$ track the mean and the variance of the summed inputs within the layer, and γ_l and β_l compute adaptive normalization parameters controlled by the latent vector derived from **z**. $\odot$ is the element-wise dot product.

Implicit Neural Representation for Patch Generation. We use an implicit neural representation [39, 34, 49, 46] to learn a continuous mapping from a patch embedding $\mathbf{y}^i \in \mathbb{R}^D$ to patch pixel values $\mathbf{x}_p^i \in \mathbb{R}^{P^2 \times C}$. When coupled with Fourier features [49] or sinusoidal activation functions [46], implicit representations can constrain the space of generated samples to the space of smooth-varying natural signals. Concretely, similarly to [1], $\mathbf{x}_p^i = f_\theta(\mathbf{E}_{fou}, \mathbf{y}^i)$ where $\mathbf{E}_{fou} \in \mathbb{R}^{P^2 \cdot D}$ is a Fourier encoding of $P \times P$ spatial locations and $f_\theta(\cdot, \cdot)$ is a 2-layer MLP. For details, please refer to B. We find implicit representation to be particularly helpful for training GANs with ViT-based generators, *c.f.* Table 3a.

It is noteworthy that the generator and discriminator can have different image grids and thus different sequence lengths. We find that it is often sufficient to increase the sequence length or feature dimension of only the discriminator when scaling our model to higher resolution images.

Architecture	Conv	Pool	CIFAR		CelebA		LSUN Bedroom	
			FID ↓	IS ↑	FID ↓	IS ↑	FID ↓	IS ↑
BigGAN [6] + DiffAug [59]	✓	✓	8.59*	9.25*	-	-	-	-
StyleGAN2 [27]	✓	✓	11.1*	9.18*	**3.39**	**3.43**	3.25	**2.45**
TransGAN-XL [23]	✗	✓	11.9*	8.63*	-	-	-	-
Vanilla-ViT	✗	✗	12.7	8.40	20.2	2.57	218.1	2.20
ViTGAN (Ours)	✗	✗	**6.66**	**9.30**	3.74	3.21	**2.65**	2.36

Table 1: **Comparison to representative GAN architectures on unconditional image generation benchmarks.** *Results from the original papers. All other results are our replications. 'Conv', and 'Pool' stand for convolution, and pooling (*i.e.*, downsampling), respectively. ↓ means lower is better. ↑ means higher is better.

5 Experiments

5.1 Experiment Setup

Datasets. The **CIFAR-10** dataset [30] is a standard benchmark for image generation, containing 50K training images and 10K test images. Inception score (IS) [44] and Fréchet Inception Distance (FID) [20] are computed over the 50K images. The **LSUN bedroom** dataset [56] is a large-scale image generation benchmark, consisting of ∼3 million training images and 300 images for validation. On this dataset, FID is computed against the training set due to the small validation set. The **CelebA** dataset [32] comprises 162,770 unlabeled face images and 19,962 test images. By default, we generate 32×32 images on the CIFAR dataset and 64×64 images on the other two datasets.

Implementation Details. For 32×32 resolution, we use a 4-block ViT-based discriminator and a 4-block ViT-based generator. For 64×64 resolution, we increase the number of blocks to 6. Following ViT-Small [15], the input/output feature dimension is 384 for all Transformer blocks, and the MLP hidden dimension is 1,536. Unlike [15], we choose the number of attention heads to be 6. We find increasing the number of heads does not improve GAN training. For 32×32 resolution, we use patch size 4×4, yielding a sequence length of 64 patches. For 64×64 resolution, we simply increase the patch size to 8×8, keeping the same sequence length as in 32×32 resolution.

Translation, Color, Cutout, Scaling data augmentations [59, 25] are applied with probability 0.8. All baseline transformer-based GAN models, including ours, use balanced consistency regularization (bCR) with $\lambda_{real} = \lambda_{fake} = 10.0$. Other than bCR, we do not employ regularization methods typically used for training ViTs [51] such as Dropout, weight decay, or Stochastic Depth. We found that LeCam regularization [53], similar to bCR, improves the performance. But for clearer ablation, we do not include the LeCam regularization. We train our models with Adam with $\beta_1 = 0.0$, $\beta_2 = 0.99$, and a learning rate of 0.002 following the practice of [27]. In addition, we employ non-saturating logistic loss [18], exponential moving average of generator weights [24], and equalized learning rate [24]. We use a mini-batch size of 128.

Both ViTGAN and StyleGAN2 are based on Tensorflow 2 implementation [36]. We train our models on Google Cloud TPU v2-32 and v3-8.

5.2 Main Results

Table 1 shows the main results on three standard benchmarks for image synthesis. Our method is compared with the following baseline architectures. *TransGAN* [23] is the only existing convolution-free GAN that is entirely built on the Transformer architecture. Its best variant TransGAN-XL is compared. *Vanilla-ViT* is a ViT-based GAN that employs the generator illustrated in Fig. 2 (A) and a vanilla ViT discriminator without any techniques discussed in Section 4.1. For fair comparison, R1 penalty and bCR [60] + DiffAug [59] were used for this baseline. The architecture with the generator illustrated in Fig. 2 (B) is separately compared in Table 3a. In addition, BigGAN [6] and StyleGAN2 [27] are also included as state-of-the-art CNN-based GAN models.
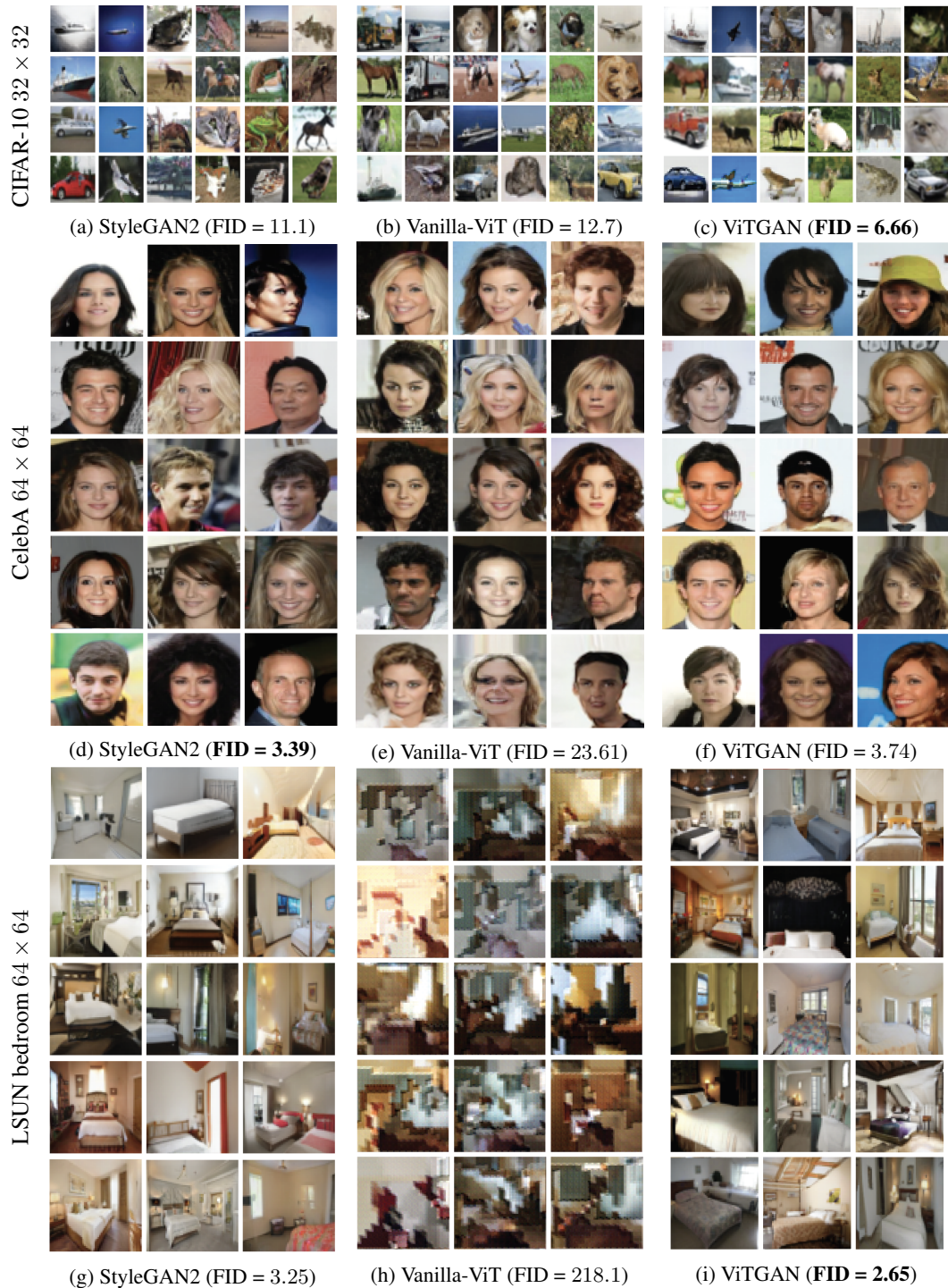
Figure 3: **Qualitative Comparison.** We compare our ViTGAN with StyleGAN2, and our best Transformer baseline, *i.e.*, a vanilla pair of ViT generator and discriminator described in Section 5.2, on the CIFAR-10 32×32, CelebA 64×64 and LSUN Bedroom 64×64 datasets.
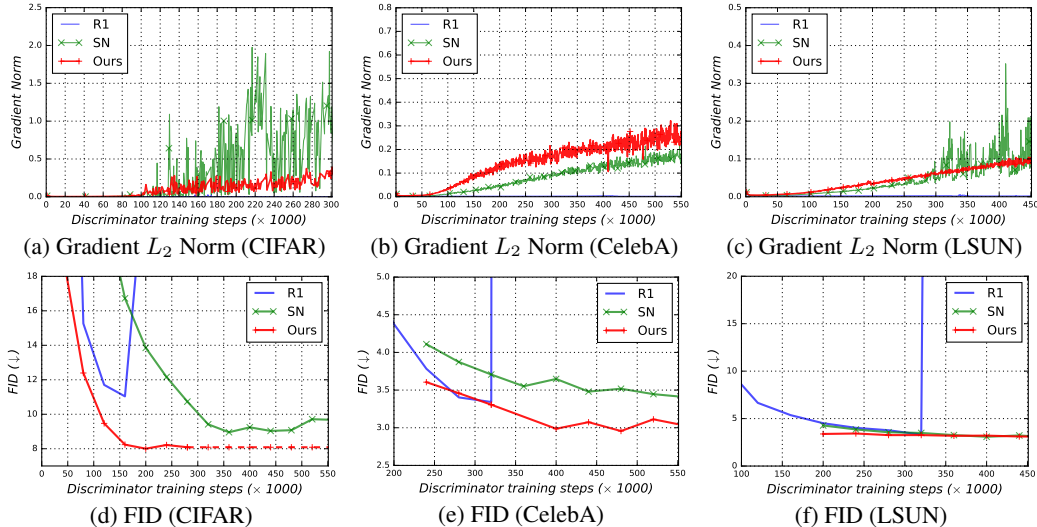
Figure 4: **(a-c) Gradient magnitude (L_2 norm over all parameters) of ViT discrminator and (d-f) FID score (lower the better)** as a function of training iteration. Our ViTGAN are compared with two baselines of Vanilla ViT discriminators with R1 penalty and spectral norm (SN). The remaining architectures are the same for all methods. Our method overcomes the spikes of gradient magnitude, and achieve significantly lower FIDs (*i.e.* on CIFAR and CelebA) or a comparable FID (*i.e.* on LSUN). All experiments here are conducted with 6-block ViTGAN generator networks on 32×32 resolution.

Our ViTGAN model outperforms other Transformer-based GAN models by a large margin. This results from the improved stable GAN training on the Transformer architecture, as shown in Fig. 4. It achieves comparable performance to the state-of-the-art CNN-based models. This result provides an empirical evidence that Transformer architectures may rival convolutional networks in generative adversarial training. Note that in Table 1 to focus on comparing the architectures, we use a generic version of StyleGAN2. More comprehensive comparisons with StyleGAN2 with data augmentation (*e.g.* [59, 25]) are included in Appendix A.1.

As shown in Fig. 3, the image fidelity of the best Transformer baseline (Middle Row) has been notably improved by the proposed ViTGAN model (Last Row). Even compared with StyleGAN2, ViTGAN generates images with comparable quality and diversity. Notice there appears to be a perceivable difference between the images generated by Transformers and CNNs, *e.g.* in the background of the CelebA images. Both the quantitative results and qualitative comparison substantiate the efficacy of the proposed ViTGAN as a competitive Transformer-based GAN model.

5.3 Ablation Studies

We conduct ablation experiments on the CIFAR dataset to study the contributions of the key techniques and verify the design choices in our model.

Compatibility with CNN-based GAN   In Table 2, we mix and match the generator and discriminator of our ViTGAN and the leading CNN-based GAN: StyleGAN2. With the StyleGAN2 generator, our ViTGAN discriminator outperforms the vanilla ViT discriminator. Besides, our ViTGAN generator still works together with the StyleGAN2 discriminator. The results show the proposed techniques are compatible with both Transformer-based and CNN-based generators and discriminators.

Generator architecture   Table 3a shows GAN performances under three different generator architectures, as shown in Figure 2. Fig. 2 (B) underperforms other architectures. We find that Fig. 2 (A) works well but lags behind Fig. 2 (C) due to its instability. Regarding mapping between patch embedding and pixel, it seems consistently better to use implicit neural representation (denoted as NeurRep in Table 3a) than linear mapping. This observation substantiates our claim that implicit neural representation benefits for training GANs with ViT-based generators.

8

Generator	Discriminator	FID ↓	IS ↑
ViTGAN	ViTGAN	6.66	9.30
StyleGAN2	StyleGAN2	5.60	9.41
StyleGAN2	Vanilla-ViT	17.3	8.57
StyleGAN2	ViTGAN	10.2	9.08
ViTGAN	StyleGAN2	**4.57**	**9.89**

Table 2: **Comparison of transformer-based GANs on CIFAR-10**. Even paired with CNN generators or discriminators, our mixed ViTGAN can still achieve comparable performance on CIFAR-10. All the models are trained with bCR [60] + DiffAug [59].

Discriminator regularization   Table 3b validates the necessity of the techniques discussed in Section 4.1. First, we compare GAN performances under different regularization methods. Training GANs with ViT discriminator under R1 penalty [33] is highly unstable, as shown in Figure 4, sometimes resulting in complete training failure (indicated as IS=NaN in Row 1 of Table 3b). Spectral normalization (SN) is better than R1 penalty. But SN still exhibits high-variance gradients and therefore suffers from low quality scores. Our L_2+ISN regularization improves the stability significantly ($c.f.$ Fig. 4) and achieves the best IS and FID scores as a consequence. On the other hand, the overlapping patch is a simple trick that yields further improvement over the L_2+ISN method. However, the overlapping patch by itself does not work well (see a comparison between Row 3 and 9). The above results validate the essential role of these techniques in achieving the final performance of the ViTGAN model.

w Embedding	Output Mapping	FID ↓	IS ↑
Fig 2 (A)	Linear	14.3	8.60
Fig 2 (A)	NeurRep	11.3	9.05
Fig 2 (B)	Linear	328	1.01
Fig 2 (B)	NeurRep	285	2.46
Fig 2 (C)	Linear	15.1	8.58
Fig 2 (C)	NeurRep	**6.66**	**9.30**

(a) **Generator Ablation Studies.** NeurRep denotes implicit neural representation.

Aug.	Reg.	Overlap	FID ↓	IS ↑
✗	R1	✗	2e4	NaN
✗	R1	✓	129	4.99
✓	R1	✓	13.1	8.71
✗	SN	✗	121	4.28
✓	SN	✗	10.2	8.78
✓	L_2+SN	✗	168	2.36
✓	ISN	✗	8.51	9.12
✓	L_2+ISN	✗	8.36	9.02
✓	L_2+ISN	✓	**6.66**	**9.30**

(b) **Discriminator Ablation Studies.** 'Aug.', 'Reg.', and 'Overlap' stand for DiffAug [59] + bCR [60], and regularization method, and overlapping image patches, respectively.

Table 3: **Ablation studies of ViTGAN on CIFAR-10. Left:** the ablation studies of the **generator architecture** options on CIFAR-10. **Right:** the ablation studies of **discriminator regularization** on CIFAR-10.

6   Conclusion

We have introduced ViTGAN, leveraging Vision Transformers (ViTs) in GANs, and proposed essential techniques to ensuring its training stability and improving its convergence. Our experiments on standard benchmarks (CIFAR-10, CelebA, and LSUN bedroom) demonstrate that the presented model achieves comparable performance to state-of-the-art CNN-based GANs. Regarding the limitation, ViTGAN is a new generic GAN model built on vanilla ViT architecture. It still cannot beat the best available CNN-based GAN model with sophisticated techniques developed over years. This could be improved by incorporating advanced training techniques ($e.g.$, [22, 45]) into the ViTGAN framework. We hope that ViTGAN can facilitate future research in this area and could be extended to other image [21, 40] and video [54, 43] synthesis tasks.

Acknowledgments

References

[1] Ivan Anokhin, Kirill Demochkin, Taras Khakhulin, Gleb Sterkin, Victor Lempitsky, and Denis Korzhenkov. Image generators with conditionally-independent pixel synthesis. In *CVPR*, 2021.

[2] Martin Arjovsky, Soumith Chintala, and Léon Bottou. Wasserstein generative adversarial networks. In *ICML*, 2017.

[3] Anurag Arnab, Mostafa Dehghani, Georg Heigold, Chen Sun, Mario Lučić, and Cordelia Schmid. Vivit: A video vision transformer. *arXiv preprint arXiv:2103.15691*, 2021.

[4] Josh Beal, Eric Kim, Eric Tzeng, Dong Huk Park, Andrew Zhai, and Dmitry Kislyuk. Toward transformer-based object detection. *arXiv preprint arXiv:2012.09958*, 2020.

[5] Gedas Bertasius, Heng Wang, and Lorenzo Torresani. Is space-time attention all you need for video understanding? *arXiv preprint arXiv:2102.05095*, 2021.

[6] Andrew Brock, Jeff Donahue, and Karen Simonyan. Large scale gan training for high fidelity natural image synthesis. In *ICLR*, 2019.

[7] Tom Brown, Benjamin Mann, Nick Ryder, Melanie Subbiah, Jared D Kaplan, Prafulla Dhariwal, Arvind Neelakantan, Pranav Shyam, Girish Sastry, Amanda Askell, Sandhini Agarwal, Ariel Herbert-Voss, Gretchen Krueger, Tom Henighan, Rewon Child, Aditya Ramesh, Daniel Ziegler, Jeffrey Wu, Clemens Winter, Chris Hesse, Mark Chen, Eric Sigler, Mateusz Litwin, Scott Gray, Benjamin Chess, Jack Clark, Christopher Berner, Sam McCandlish, Alec Radford, Ilya Sutskever, and Dario Amodei. Language models are few-shot learners. In *NeurIPS*, 2020.

[8] Hanting Chen, Yunhe Wang, Tianyu Guo, Chang Xu, Yiping Deng, Zhenhua Liu, Siwei Ma, Chunjing Xu, Chao Xu, and Wen Gao. Pre-trained image processing transformer. In *ICML*, 2020.

[9] Mark Chen, Alec Radford, Rewon Child, Jeff Wu, Heewoo Jun, Prafulla Dhariwal, David Luan, and Ilya Sutskever. Generative pretraining from pixels. In *ICML*, 2020.

[10] Ting Chen, Mario Lucic, Neil Houlsby, and Sylvain Gelly. On self modulation for generative adversarial networks. In *ICLR*, 2019.

[11] Xinlei Chen, Saining Xie, and Kaiming He. An empirical study of training self-supervised vision transformers. *CoRR*, abs/2104.02057, 2021.

[12] Jean-Baptiste Cordonnier, Andreas Loukas, and Martin Jaggi. Multi-head attention: Collaborate instead of concatenate, 2020.

[13] Jacob Devlin, Ming-Wei Chang, Kenton Lee, and Kristina Toutanova. Bert: Pre-training of deep bidirectional transformers for language understanding. In *ACL*, 2019.

[14] Yihe Dong, Jean-Baptiste Cordonnier, and Andreas Loukas. Attention is not all you need: Pure attention loses rank doubly exponentially with depth. *arXiv preprint arXiv:2103.03404*, 2021.

[15] Alexey Dosovitskiy, Lucas Beyer, Alexander Kolesnikov, Dirk Weissenborn, Xiaohua Zhai, Thomas Unterthiner, Mostafa Dehghani, Matthias Minderer, Georg Heigold, Sylvain Gelly, Jakob Uszkoreit, and Neil Houlsby. An image is worth 16x16 words: Transformers for image recognition at scale. In *ICLR*, 2021.

[16] Patrick Esser, Robin Rombach, and Björn Ommer. Taming transformers for high-resolution image synthesis. In *CVPR*, 2021.

[17] William Fedus, Mihaela Rosca, Balaji Lakshminarayanan, Andrew M. Dai, Shakir Mohamed, and Ian J. Goodfellow. Many paths to equilibrium: Gans do not need to decrease a divergence at every step. In *ICLR*, 2018.

[18] Ian Goodfellow, Jean Pouget-Abadie, Mehdi Mirza, Bing Xu, David Warde-Farley, Sherjil Ozair, Aaron Courville, and Yoshua Bengio. Generative adversarial nets. In *NeurIPS*, 2014.

[19] Ishaan Gulrajani, Faruk Ahmed, Martin Arjovsky, Vincent Dumoulin, and Aaron Courville. Improved training of wasserstein gans. In *NeurIPS*, 2017.

[20] Martin Heusel, Hubert Ramsauer, Thomas Unterthiner, Bernhard Nessler, and Sepp Hochreiter. Gans trained by a two time-scale update rule converge to a local nash equilibrium. In *NeurIPS*, 2017.

[21] Phillip Isola, Jun-Yan Zhu, Tinghui Zhou, and Alexei A Efros. Image-to-image translation with conditional adversarial networks. In *CVPR*, 2017.

[22] Jongheon Jeong and Jinwoo Shin. Training {gan}s with stronger augmentations via contrastive discriminator. In *ICLR*, 2021.

[23] Yifan Jiang, Shiyu Chang, and Zhangyang Wang. Transgan: Two transformers can make one strong gan. *arXiv preprint arXiv:2102.07074*, 2021.

[24] Tero Karras, Timo Aila, Samuli Laine, and Jaakko Lehtinen. Progressive growing of gans for improved quality, stability, and variation. In *ICLR*, 2018.

[25] Tero Karras, Miika Aittala, Janne Hellsten, Samuli Laine, Jaakko Lehtinen, and Timo Aila. Training generative adversarial networks with limited data. In *NeurIPS*, 2020.

[26] Tero Karras, Samuli Laine, and Timo Aila. A style-based generator architecture for generative adversarial networks. In *CVPR*, 2019.

[27] Tero Karras, Samuli Laine, Miika Aittala, Janne Hellsten, Jaakko Lehtinen, and Timo Aila. Analyzing and improving the image quality of StyleGAN. In *CVPR*, 2020.

[28] Hyunjik Kim, George Papamakarios, and Andriy Mnih. The lipschitz constant of self-attention. In *ICML*, 2021.

[29] Naveen Kodali, Jacob Abernethy, James Hays, and Zsolt Kira. On convergence and stability of gans. *arXiv preprint arXiv:1705.07215*, 2017.

[30] Alex Krizhevsky, Geoffrey Hinton, et al. Learning multiple layers of features from tiny images. Technical report, Citeseer, 2009.

[31] Y. LeCun, B. Boser, J. S. Denker, D. Henderson, R. E. Howard, W. Hubbard, and L. D. Jackel. Backpropagation applied to handwritten zip code recognition. *Neural Computation*, 1(4):541–551, 1989.

[32] Ziwei Liu, Ping Luo, Xiaogang Wang, and Xiaoou Tang. Deep learning face attributes in the wild. In *ICCV*, 2015.

[33] Lars Mescheder, Sebastian Nowozin, and Andreas Geiger. Which training methods for gans do actually converge? In *ICML*, 2018.

[34] Lars Mescheder, Michael Oechsle, Michael Niemeyer, Sebastian Nowozin, and Andreas Geiger. Occupancy networks: Learning 3d reconstruction in function space. In *CVPR*, 2019.

[35] Takeru Miyato, Toshiki Kataoka, Masanori Koyama, and Yuichi Yoshida. Spectral normalization for generative adversarial networks. In *ICLR*, 2018.

[36] mookyung song. stylegan2-tf-2.x. `https://github.com/moono/stylegan2-tf-2.x,`, 2020.

[37] Alfred Müller. Integral probability metrics and their generating classes of functions. *Advances in Applied Probability*, pages 429–443, 1997.

[38] Sebastian Nowozin, Botond Cseke, and Ryota Tomioka. f-gan: Training generative neural samplers using variational divergence minimization. In *NeurIPS*, 2016.

[39] Jeong Joon Park, Peter Florence, Julian Straub, Richard Newcombe, and Steven Lovegrove. Deepsdf: Learning continuous signed distance functions for shape representation. In *CVPR*, 2019.

[40] Gaurav Parmar, Dacheng Li, Kwonjoon Lee, and Zhuowen Tu. Dual contradistinctive generative autoencoder. In *CVPR*, 2021.

[41] Aditya Ramesh, Mikhail Pavlov, Gabriel Goh, Scott Gray, Chelsea Voss, Alec Radford, Mark Chen, and Ilya Sutskever. Zero-shot text-to-image generation. *arXiv preprint arXiv:2102.12092*, 2021.

[42] René Ranftl, Alexey Bochkovskiy, and Vladlen Koltun. Vision transformers for dense prediction. *ArXiv preprint*, 2021.

[43] Masaki Saito, Shunta Saito, Masanori Koyama, and S. Kobayashi. Train sparsely, generate densely: Memory-efficient unsupervised training of high-resolution temporal gan. *International Journal of Computer Vision*, 2020.

[44] Tim Salimans, Ian Goodfellow, Wojciech Zaremba, Vicki Cheung, Alec Radford, and Xi Chen. Improved techniques for training gans. In *NeurIPS*, 2016.

[45] Edgar Schonfeld, Bernt Schiele, and Anna Khoreva. A u-net based discriminator for generative adversarial networks. In *CVPR*, 2020.

[46] Vincent Sitzmann, Julien N.P. Martel, Alexander W. Bergman, David B. Lindell, and Gordon Wetzstein. Implicit neural representations with periodic activation functions. In *NeurIPS*, 2020.

[47] Jiaming Song and Stefano Ermon. Bridging the gap between f-gans and wasserstein gans. In *ICML*, 2020.

[48] Robin Strudel, Ricardo Garcia, Ivan Laptev, and Cordelia Schmid. Segmenter: Transformer for semantic segmentation. *arXiv preprint arXiv:2105.05633*, 2021.

[49] Matthew Tancik, Pratul P. Srinivasan, Ben Mildenhall, Sara Fridovich-Keil, Nithin Raghavan, Utkarsh Singhal, Ravi Ramamoorthi, Jonathan T. Barron, and Ren Ng. Fourier features let networks learn high frequency functions in low dimensional domains. In *NeurIPS*, 2020.

[50] Ilya Tolstikhin, Neil Houlsby, Alexander Kolesnikov, Lucas Beyer, Xiaohua Zhai, Thomas Unterthiner, Jessica Yung, Daniel Keysers, Jakob Uszkoreit, Mario Lucic, et al. Mlp-mixer: An all-mlp architecture for vision. *arXiv preprint arXiv:2105.01601*, 2021.

[51] Hugo Touvron, Matthieu Cord, Matthijs Douze, Francisco Massa, Alexandre Sablayrolles, and Hervé Jégou. Training data-efficient image transformers & distillation through attention. *arXiv preprint arXiv:2012.12877*, 2020.

[52] Ngoc-Trung Tran, Viet-Hung Tran, Ngoc-Bao Nguyen, Trung-Kien Nguyen, and Ngai-Man Cheung. On data augmentation for gan training. *IEEE Transactions on Image Processing*, 30:1882–1897, 2021.

[53] Hung-Yu Tseng, Lu Jiang, Ce Liu, Ming-Hsuan Yang, and Weilong Yang. Regularizing generative adversarial networks under limited data. In *CVPR*, 2021.

[54] Sergey Tulyakov, Ming-Yu Liu, Xiaodong Yang, and Jan Kautz. MoCoGAN: Decomposing motion and content for video generation. In *CVPR*, 2018.

[55] Ashish Vaswani, Noam Shazeer, Niki Parmar, Jakob Uszkoreit, Llion Jones, Aidan N Gomez, Łukasz Kaiser, and Illia Polosukhin. Attention is all you need. In *NeurIPS*, 2017.

[56] Fisher Yu, Yinda Zhang, Shuran Song, Ari Seff, and Jianxiong Xiao. Lsun: Construction of a large-scale image dataset using deep learning with humans in the loop. *arXiv preprint arXiv:1506.03365*, 2015.

[57] Han Zhang, Ian J. Goodfellow, Dimitris N. Metaxas, and Augustus Odena. Self-attention generative adversarial networks. In *ICML*, 2019.

[58] Han Zhang, Zizhao Zhang, Augustus Odena, and Honglak Lee. Consistency regularization for generative adversarial networks. In *ICLR*, 2020.

[59] Shengyu Zhao, Zhijian Liu, Ji Lin, Jun-Yan Zhu, and Song Han. Differentiable augmentation for data-efficient gan training. In *NeurIPS*, 2020.

[60] Zhengli Zhao, Sameer Singh, Honglak Lee, Zizhao Zhang, Augustus Odena, and Han Zhang. Improved consistency regularization for gans. In *AAAI*, 2021.

[61] Zhengli Zhao, Zizhao Zhang, Ting Chen, Sameer Singh, and Han Zhang. Image augmentations for GAN training. *arXiv preprint:2006.02595*, 2020.

[62] Zhiming Zhou, Jiadong Liang, Yuxuan Song, Lantao Yu, Hongwei Wang, Weinan Zhang, Yong Yu, and Zhihua Zhang. Lipschitz generative adversarial nets. In *ICML*, 2019.

A More Quantitative Results

A.1 Effects of Data Augmentation

Table 4 presents the comparison of the Convolution-based GAN architectures (BigGAN and Style-GAN2) and our Transformer-based architecture (ViTGAN). This table complements the results in Table 1 of the main paper by a closer examination of the network architecture performance with and without using data augmentation. The differentiable data augmentation (DiffAug) [59] is used in this study.

As shown, data augmentation plays a more critical role in ViTGAN. This is not unexpected because discriminators built on Transformer architectures are more capable of over-fitting or memorizing the data. DiffAug increases the diversity of the training data, thereby mitigating the overfitting issue in adversarial training. Nevertheless, with DiffAug, ViTGAN performs comparably to the leading-performing CNN-based GAN models: BigGAN and StyleGAN2.

In addition, Table 4 includes the model performance without using the balanced consistency regularization (bCR) [60].

Method	Data Augmentation	Conv	FID $\downarrow$	IS $\uparrow$
BigGAN	None	Y	9.59	9.06
BigGAN	DiffAug	Y	8.59	9.25
StyleGAN2	None	Y	11.1	9.18
StyleGAN2	DiffAug	Y	9.89	9.40
ViTGAN	None	N	30.72	7.75
ViTGAN	DiffAug	N	6.66	9.30
ViTGAN w/o. bCR	DiffAug	N	8.84	9.02

Table 4: Effectiveness of data augmentation and regularization on the CIFAR-10 dataset.

B Implementation Notes

Patch Extraction   We use a simple trick to mitigate over-fitting of the ViT-based discriminator by allowing some overlap between image patches. For each border edge of the patch, we extend it by o pixels, making the effective patch size $(P + 2o) \times (P + 2o)$, where $o = \frac{P}{2}$. Although this operation has a connection to a convolution operation with kernel $(P + 2o) \times (P + 2o)$ and stride $P \times P$, we do not regard it as a convolution operator in our model because of the fact that we do not use convolution in our implementation. Note that the extraction of (non-overlapping) patches in the Vanilla ViT [15] also has a connection to a convolution operation with kernel $P \times P$ and stride $P \times P$.

Positional Embedding   Each positional embedding of ViT networks is a linear projection of patch position followed by a sine activation function. The patch positions are normalized to lie between -1.0 and 1.0.

Implicit Neural Representation for Patch Generation   Each positional embedding is a linear projection of pixel coordinate followed by a sine activation function (hence the name Fourier encoding). The pixel coordinates for P^2 pixels are normalized to lie between -1.0 and 1.0. The 2-layer MLP takes positional embedding $\mathbf{E}_{fou}$ as its input, and it is conditioned on patch embedding $\mathbf{y}^i$ via weight modulation as in [27, 1].